REPORT DOCUMENTATION PAGE		Form Approved OMB No. 0704-0188

1. REPORT DATE (DD-MM-YYYY)	2. REPORT TYPE	3. DATES COVERED (From - To)
02-08-2011	Conference Proceeding	

4. TITLE AND SUBTITLE	
Merging Imagery and Models for River Current Prediction	5a. CONTRACT NUMBER
	5b. GRANT NUMBER
	5c. PROGRAM ELEMENT NUMBER 0602435N
6. AUTHOR(S) Cheryl Ann Blain, Robert Linzell and Paul McKay	5d. PROJECT NUMBER
	5e. TASK NUMBER
	5f. WORK UNIT NUMBER 73-6527-A1-5
7. PERFORMING ORGANIZATION NAME(S) AND ADDRESS(ES) Naval Research Laboratory, Oceanography Division, Stennis Space Center, MS 39529-5004	8. PERFORMING ORGANIZATION REPORT NUMBER NRL/PP/7320--11-0661
9. SPONSORING/MONITORING AGENCY NAME(S) AND ADDRESS(ES) Office of Naval Research, 800 N. Quincy St., Arlington, VA 22217-5660	10. SPONSOR/MONITOR'S ACRONYM(S) ONR
	11. SPONSOR/MONITOR'S REPORT NUMBER(S)

12. DISTRIBUTION/AVAILABILITY STATEMENT
Approved for public release, distribution is unlimited.

20110829009

13. SUPPLEMENTARY NOTES

14. ABSTRACT
To meet the challenge of operating in river environments with denied access and to improve the riverine intelligence available to the warfighter, advanced high resolution river circulation models are combined with remote sensing feature extraction algorithms to produce a predictive capability for currents and water levels in rivers where a priori knowledge of the river environment is limited. A River Simulation Tool (RST) is developed to facilitate the rapid configuration of a river model. River geometry is extracted from the automated processing of available imagery while minimal user input is collected to complete the parameter and forcing specifications necessary to configure a river model. Contingencies within the RST accommodate missing data such as a lack of water depth information and allow for ensemble computations. Successful application of the RST to river environments is demonstrated for the Snohomish River, WA. Modeled currents compare favorably to in-situ currents reinforcing the value of the developed approach.

15. SUBJECT TERMS
rivers, currents, models, edge detection, shoreline extraction, imagery, Snohomish River

16. SECURITY CLASSIFICATION OF: a. REPORT	b. ABSTRACT	c. THIS PAGE	17. LIMITATION OF ABSTRACT	18. NUMBER OF PAGES	19a. NAME OF RESPONSIBLE PERSON
Unclassified	Unclassified	Unclassified	UL	15	Cheryl Ann Blain
					19b. TELEPHONE NUMBER (Include area code) 228-688-5450

Merging Imagery and Models for River Current Prediction

Cheryl Ann Blain[a], Robert S. Linzell[b], and Paul McKay[a]

[a]Oceanography Division, Naval Research Laboratory, Stennis Space Center, MS, USA
[b]QinetiQ North America, Technology Solutions Group, Stennis Space Center, MS, USA

ABSTRACT

To meet the challenge of operating in river environments with denied access and to improve the riverine intelligence available to the warfighter, advanced high resolution river circulation models are combined with remote sensing feature extraction algorithms to produce a predictive capability for currents and water levels in rivers where *a priori* knowledge of the river environment is limited. A River Simulation Tool (RST) is developed to facilitate the rapid configuration of a river model. River geometry is extracted from the automated processing of available imagery while minimal user input is collected to complete the parameter and forcing specifications necessary to configure a river model. Contingencies within the RST accommodate missing data such as a lack of water depth information and allow for ensemble computations. Successful application of the RST to river environments is demonstrated for the Snohomish River, WA. Modeled currents compare favorably to in-situ currents reinforcing the value of the developed approach.

Keywords: rivers, currents, models, edge detection, shoreline extraction, imagery, Snohomish River

1. INTRODUCTION

River operations are rapidly becoming a major part of Military Special Operations, yet rivers pose one of the most challenging environments to characterize. Further compounding the problem is the inaccessibility of global rivers, particularly those of military interest. Their geometric complexity and continually changing position and character are difficult to measure under optimal circumstances. However it is these details pertaining to the river bank position, bed elevation, upstream discharge, and downstream water level modulation that are necessary to initialize accurate predictive river models. To meet the challenge and improve riverine intelligence available to the warfighter, advanced high resolution river circulation models are combined with remote sensing feature extraction algorithms to produce a predictive capability for currents and water levels in rivers where *a priori* knowledge of the river environment is limited.

Imagery for a specific river is typically the most recent and readily available source of information for that river. A River Simulation Tool (RST) is developed to facilitate the rapid configuration of a river model using information obtained from that single image. An automated technique within the RST has been developed that extracts river geometry and creates a computational mesh using the imagery-derived information. This mesh forms the basis of the two-dimensional river model. Additional, yet minimal, input for the RST is collected from the user to facilitate specification of upstream and downstream forcing and frictional effects of the stream bed. The RST then completes the parameter and forcing specifications required for complete configuration of a river model. Very often, water depth along a river reach viewed from imagery is unknown. For this situation, the RST generates a reasonable synthetic bathymetry based on a predefined cross-section profile relationship. Other features exist within the RST to edit derived shorelines and meshes, as well as to generate multiple realizations of the model configured from a single image. Application of the RST to river environments as diverse as the Pearl River, LA, the Atchafalaya River, LA, the Snohomish River, WA and most recently the Kootenai River, ID have been undertaken. Presented here are details of the river model configuration for the Snohomish River as derived

Further author information: (Send correspondence to C.A.B.)
C.A.B.: E-mail: cheryl.ann.blain@nrlssc.navy.mil, Telephone: +1 228 688 5450
P.M.: E-mail: paul.mckay@nrlssc.navy.mil, Telephone: +1 228 688 5664
R.S.L.: E-mail: robert.linzell.ctr@nrlssc.navy.mil, Telephone: +1 228 688 4151

Ocean Sensing and Monitoring III, edited by Weilin W. Hou, Robert Arnone, Proc. of SPIE Vol. 8030, 80300H · © 2011 SPIE · CCC code: 0277-786X/11/$18 · doi: 10.1117/12.884100

from an application of the RST. Comparisons of currents predicted by the RST-generated model to measured in-situ currents within a reach of the Snohomish River demonstrate the value of the developed approach.

Description of the methodology developed is presented in the context of an application to the Snohomish River, WA. The manuscript begins in Section 2 with a description of the process that extracts river geometry from imagery. Configuration of the river model including the creation of synthetic bathymetry and the generation of an unstructured grid is described in Section 3. Section 4 discusses the River Simulation Tool and its integration of the image processing and model configuration operations. Validation of the river currents computed by the RST-generated model for the Snohomish River are presented in Section 5. The manuscript concludes with a brief summary in Section 6.

2. EXTRACTION OF RIVER GEOMETRY FROM IMAGERY

The extraction of river geometry is a two-step process. First the imagery is processed to obtain river edge and water point locations. Depending on the method for edge detection employed, the edge data can be a multi-pixel band of locations bracketing the shoreline of the river or, in the ideal case, a single set of points that define the shoreline. The location of pixels identified as water is the second component of the image processing. Once the edge and water data are obtained, the second step commences, the processing of edge data into an ordered, oriented list of coordinates that define both banks of the river.

2.1 Image Processing

Two approaches are developed for processing available imagery into river edge and water point locations. The first option targets imagery in the National Imagery Transmission Format (NITF). Within the developed tool, the NITF Warper Image Processing Utility,[1] river edges can be derived from either pan sharpened or multi-spectral images. Two parameters control the detection of the river edge. The first, a reduction factor, defines the amount of image sub-sampling performed prior to application of the river edge detection algorithm. The default value is set to 4. Higher reduction factors result in fewer details in the edge data, and thus, fewer edge points. For very low reduction factors, the highest detail is retained but that detail can include overhanging tree shadows which may distort the true river edge. The second parameter is a slope threshold, whose default value is 0.5. Water locations are obtained at all pixels where an applied bathymetry algorithm detects water and are not limited to locations contained within the edge data previously extracted.

Due to the occasionally limited nature of Quickbird satellite coverage or the unavailability of Quickbird in NITF format, an alternate image processing method has been developed to obtain the necessary edge and water data using imagery from other sources. The routine is designed to work with imagery from any source that is cast in a file format supported by the MATLAB® software. The best results are obtained for imagery in the visible or IR spectrum rather than multi- or hyperspectral as the presence of visible structure on the water surface can lead to confusion within the algorithm. The imagery can be of any size, though 2 m/pixel or better is a practical limit for the delineation of land and water, and the image can be in any color space, including grayscale. Imagery that qualifies includes Google Earth or Worldview 2, among others. The image processing approach is a texture-based analysis that applies thresholding to entropy calculations. The method is fully described and validated by McKay et al.[2]

The availability of measured bathymetry and observed currents,[3–5] focuses our interest on a small reach of the Snohomish River, WA shown in Fig. 1. Several images from Google Earth are tiled together (Fig. 2), forming a single image of Snohomish River, WA in the region of interest. The image of Fig. 2 is processed using the texture-based edge detection approach of McKay et al.,[2] and is visually summarized in Fig. 3. Entropy values are computed for each pixel, followed by despeckling of the image to reduce noise. Thresholding separates land (high entropy, rough texture) and water (low entropy, smooth texture) pixels and lastly, a binarized mask is applied to separately extract the edge and water point locations. The extracted edge and water point data are shown in Fig. 4. The most time consuming portion of the edge and water point extraction process is the location and tiling of all images needed to cover a desired portion of the river. For the Snohomish River, the image tiling required 6 minutes of effort while processing the edge and water point data itself consumed only two minutes, indicating a substantial degree of efficiency in the approach.

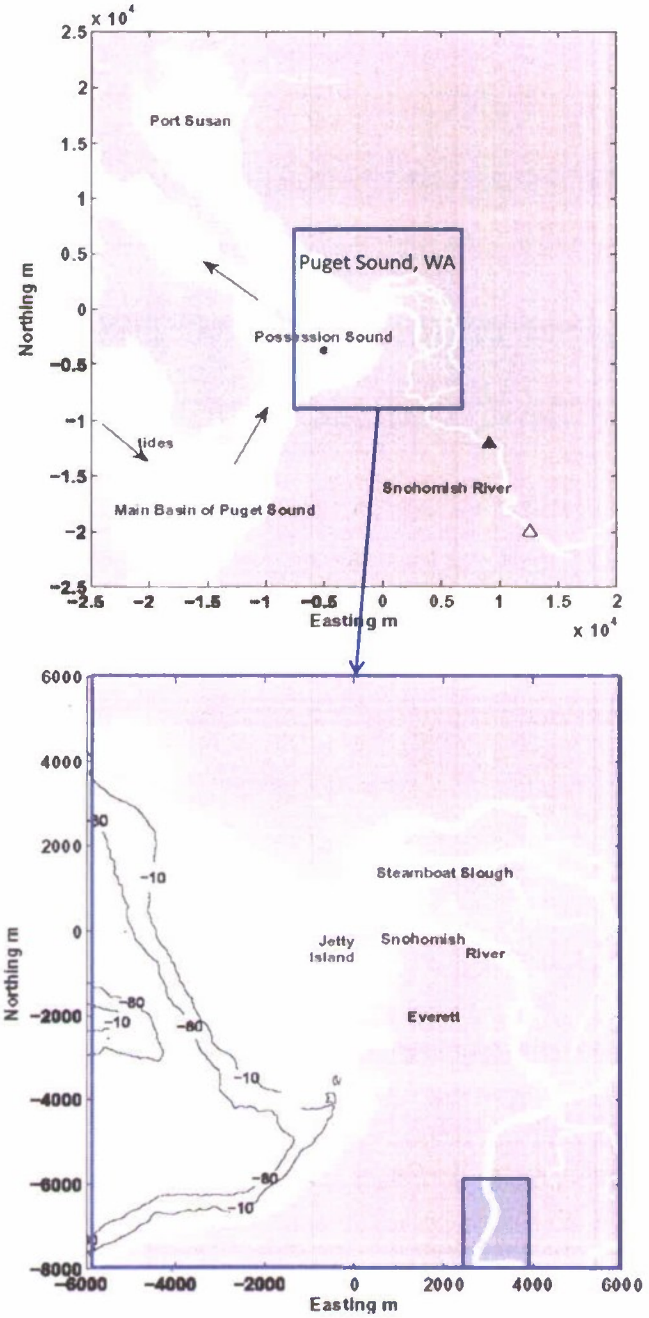

Figure 1. Reach of interest on the Snohomish River, WA.

Figure 2. Tiles images from Google Earth for the reach of interest on the Snohomish River, WA.

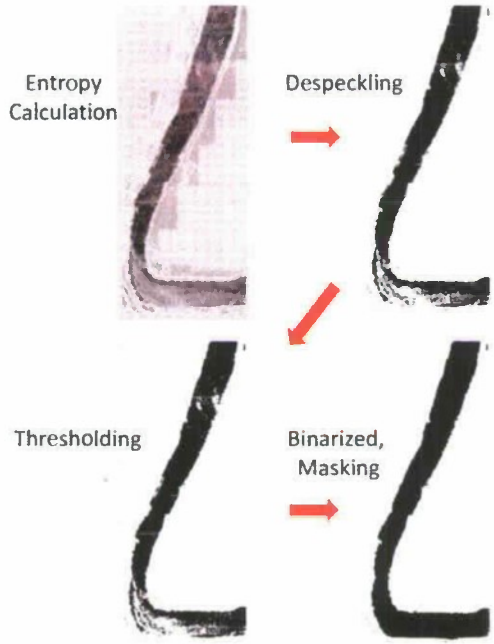

Figure 3. A depiction of the edge and water point extraction process for the Snohomish River, WA.

2.2 Shoreline Processing

Using the water and edge point data obtained from the imagery, a developed shoreline extraction procedure is performed to yield an oriented (clockwise or counter-clockwise), continuous set of shoreline coordinates that define the river geometry. The methodology is not specific to a particular source of imagery or the means by which the water and edge data are obtained. Furthermore, neither the coordinates of the water nor the edge data need be in any particular ordered sequence with respect to themselves or one another. Application of the procedure results in two segments representing each bank of the river, segments defining islands and, potentially, a smaller set of closed segments identifying isolated pockets of water that reside outside the river banks. In developing the approach, automation and simplicity are paramount. The specification of three parameters control the edge and water data processing. Their names and default values are given as: 1) the averaging box size, 5 m, 2) the maximum neighbor distance, 30 m, and 3) the maximum water point distance, 25 m. Accuracy of the final shoreline coordinates necessarily depends on the imagery source, its resolution and the processing technique(s) applied to obtain the initial water and edge data.

Details of the shoreline processing are shown schematically in Fig. 5 and described succinctly here. A moving average (box average) is applied to the set of edge points to smooth the possibly jagged band of edge pixel locations and minimize the effects of obstructions and overhanging trees represented in the edge data. The result is a set of mean edge data locations. Next, three-point segments are created from edge data points by determining the two nearest neighbor edge points within a specified radius (max. neighbor distance) of an edge point. The 3-point segments are oriented using a normal vector that points to the nearest water data point location within a specified radius (max. water point distance). A cross-product between the normal vector and the vector connecting neighboring edge points of the three-point segment are used to define the head/tail

Figure 4. The set of water (blue) and edge (red) point data extracted from imagery for the Snohomish River, WA.

connection between edge points. At this point all 3-point segments are connected head to tail by vectors whose normal is directed towards their nearest water point, creating boundary segments. Boundary segments with three or more points that have head and tail points within a specified search distance of nearest neighbors are connected. Remaining open segments are linked together by determining which segment start point is within a nearest neighbor search distance of a segment end point. Islands are identified as segments whose end point is within a specified threshold of its own starting point. The final step is to eliminate segments that do not contain a minimum number of edge points as defined by a user specified threshold. This procedure automatically filters extraneous water data and noisy edge data. The boundary segments that remain form an ordered, oriented set of shoreline data point coordinates.

3. CONFIGURATION OF THE RIVER MODEL

Essential components of a computational river model include a grid of discrete points that represent the river reach, water depths for all points in that grid, upstream and downstream forcing such as discharge and water level, and specification of the bottom sediment type so that a frictional coefficient can be determined. The model applied herein to the Snohomish River is ADCIRC,[6,7] a finite element-based model that uses unstructured meshes composed of linear triangles.

3.1 Bathymetry

Detailed information on river water depths is often unavailable or is limited in coverage. For these situations a synthetic bathymetry profile is computed for cross-sections constructed along the river. At each cross-section, a parabolic function is applied by dividing the cross-section into two halves, subdividing each half into discrete points that extend shoreward from the midpoint, and assigning to each point a depth that varies as the distance from the midpoint. Algorithmically, this synthetic bathymetry is expressed:

$$h = 1/(4p)(d - x_0)^2 + z_0 \tag{1}$$

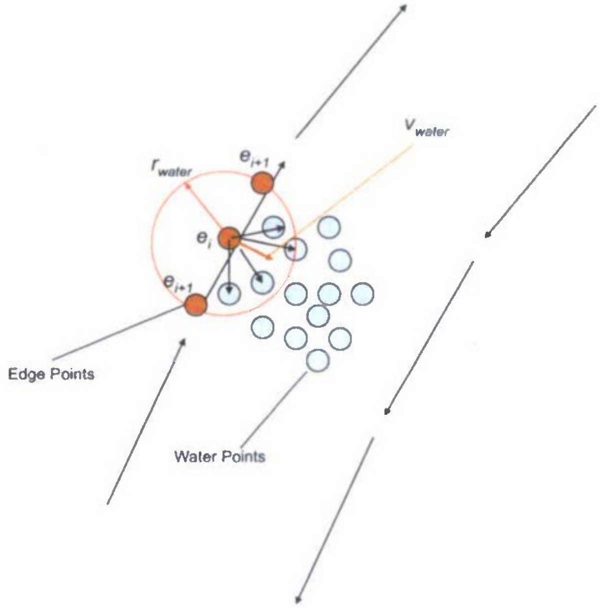

Figure 5. A graphical interpretation of the edge point connection process to form ordered, oriented shoreline coordinates.

where h is the computed depth value, x_0 is the horizontal offset, z_0 is the vertical offset, and p is the distance from the vertex of the parabola to its focus scaled by half the length of the cross-section. The expression for water depth in equation 1 is inverted to enforce a maximum depth at the vertes using the simple relation, $h = abs(max(h) - h)$. To guarantee a minimum value that is identically zero, the parabola is vertically translated using, $h = h\text{-}min(h)$, ensuring that shorelines have zero depth. The result is a smoothly varying depth profile at each cross-section with narrower stretches of river having shallower maximum depths than wider sections of the river. While this simplified representation of the bathymetry does not capture the effects of sedimentation and scour in river bends or other asymmetries associated with the dynamics of the river channel, it has proven to be a robust approach for representing mean river conditions in the absence of measured bathymetric values.

3.2 The Computational Mesh

The information required to proceed with generation of an unstructured mesh of the river reach is now available, the ordered, oriented shoreline data extracted from the imagery and water depth information over the river reach of interest. The automated finite element mesh generation utility, MeshGUI,[8] is applied to the Snohomish River. An initial coarse resolution of 50 m with two depth-based refinements provides the best balance of resolution and model performance (i.e., execution speed determined by mesh size). The resulting mesh, depicted in Fig. 6, contains 41997 nodes and 75246 triangular elements with a mean resolution of 16.7 m. The range of nodal spacing is from 6 m to 33 m. To eliminate reflection of a wave moving upstream off the upstream boundary in a limited domain model, a channel extension to the mesh at the upstream boundary is automatically constructed. The length of the extension is determined by considering the distance required for dissipation of a shallow water wave moving upstream:

$$L = E/D(gh)^{1/2} \tag{2}$$

where E is the global average tidal energy dissipation rate (4000 J/m^2), D is the dissipation rate of tidal energy in a shallow tidal plain (0.5 W/m^2) and h is the mean depth of the channel (3 m here).

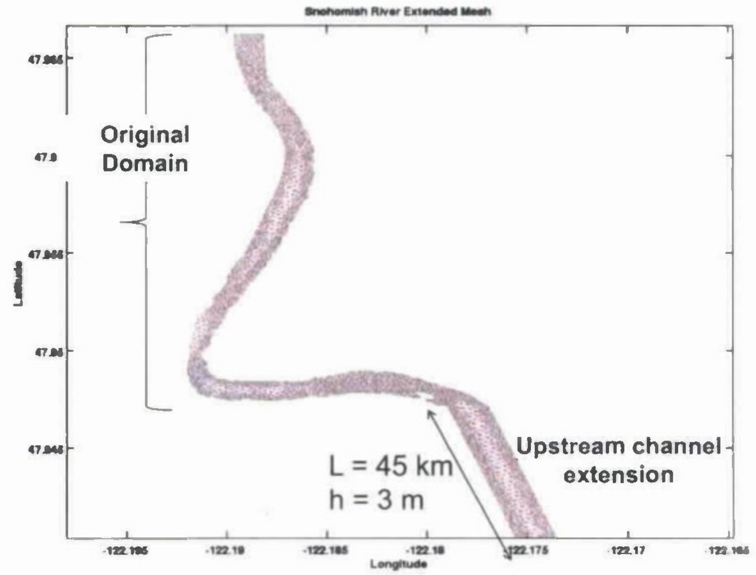

Figure 6. The finite element mesh of the Snohomish River, WA created using synthetic bathymetry and extracted edge data from imagery.

3.3 Boundary Forcing

For the Snohomish River, currents flow to the west then north-northeast emptying into the Possession Sound, the easternmost basin of Puget Sound. Upstream conditions are defined by the sum of daily discharges from the Pilchuck and Snohomish Rivers as measured by USGS gages 1215530 and 12150800, respectively. For the time period of interest in September 2009 the upstream discharge rates applied are shown in Fig. 7. The discharge rate peaks on 08 September at just over 9000 cfs and declines rapidly over the next four days until reaching a fairly constant discharge of 2000 cfs for another 10 days. Discharge drops further beyond 24 September.

Downstream the Snohomish River is influenced by the tidal modulations of Puget Sound. Tides at the Strait of Juan de Fuca, connecting the Pacific Ocean to Puget Sound, are extracted from a global tidal database, FES2004,[9] and applied at the downstream boundary of the Snohomish river model. A 13-hour lag is applied to the water level forcing to compensate for travel time from the open ocean to the river mouth.

3.4 Bed Friction

In addition to the applied physical forcing at the upstream and downstream ends of the river, frictional resistance of the bed material is another modifying force for current dynamics in the river. Bottom drag is assumed to vary as the square of the current magnitude, following a basic quadratic friction law. The type of sediment present determines the frictional coefficient. Specifically, a sediment type is related to a specified Manning's coefficient.[10] The quadratic bottom drag coefficient is then computed based on the water depth using the the Manning's and Darcy-Weisbach equations.[11] For the Snohomish River, sand (0.3 mm quartz) is selected as the sediment type for the channel bed.

4. THE RIVER SIMULATION TOOL

The process of extracting river geometry from imagery, generating a computational mesh, and configuring a river model with boundary forcing is all handled within a the developed River Simulation Tool (RST).[12] The RST is comprised of MATLAB®-based software that provides an intuitive interface for configuring a 2D hydrodynamic model of a river that has been remotely observed through imagery data. To achieve full functionality, the RST

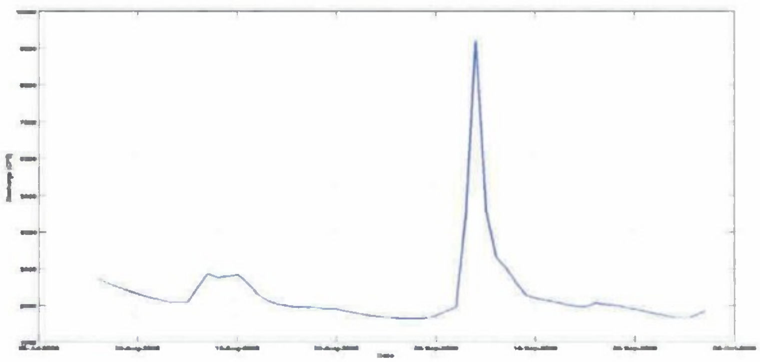

Figure 7. Upstream discharge (in cfs) applied to the Snohomish River model during the period of 9-26 September 2009.

GUI utilizes additional software tools, written in other computer programming languages such as FORTRAN and Perl. The RST is designed to be self-contained and flexible, automating as much of the image processing and mesh creation as possible if desired by the user and yet allowing user input of key pieces of information. Capabilities for interactive editing of the river shoreline or the computational mesh to the specification of model parameters and forcing are integral features of the software. At the same time the RST maintains default parameter and forcing configurations for the model as well as contingencies for specifying missing information, such as upstream forcing or bathymetry. Realizing that a great deal of uncertainty can accompany application of the RST to a real river, a capability for configuring multiple input specifications is available. From these multiple data sets an ensemble of model runs can be performed that bracket uncertainty or assess the sensitivity of predictions to unknown inputs. Execution of the river model is performed external to the RST software package.

4.1 Components and Features

The RST is comprised of six components defined by their functional goal and a visual display field that facilitates interaction and understanding within the RST. Components on the initial page of the GUI, shown in Fig. 8, are identified from top to bottom on the left side of the GUI as: *Mesh Creation* which encompasses shoreline creation, bathymetry specification and automated grid generation, *Model Input Parameters* through which bottom type and lateral mixing coefficients are specified, *Ensemble Option* for the creation of multiple model configurations based on a specific mesh and bathymetry, and *Input and Output File Naming* to customize the model run file names. A button at the top the *Mesh Creation* component labelled *Process Imagery* launches the *Image Processing* GUI which handles pixel extraction an imagery data set and processes edge and water point locations within a selected region. A secondary page of the RST GUI, *River Discharge and Tidal Forcing Input*, automatically displays at an appropriate time, and assists in the identification of open boundaries and their forcing. Detailed descriptions of the functionality and usage of each RST component is found in Blain et al 2009.[12]

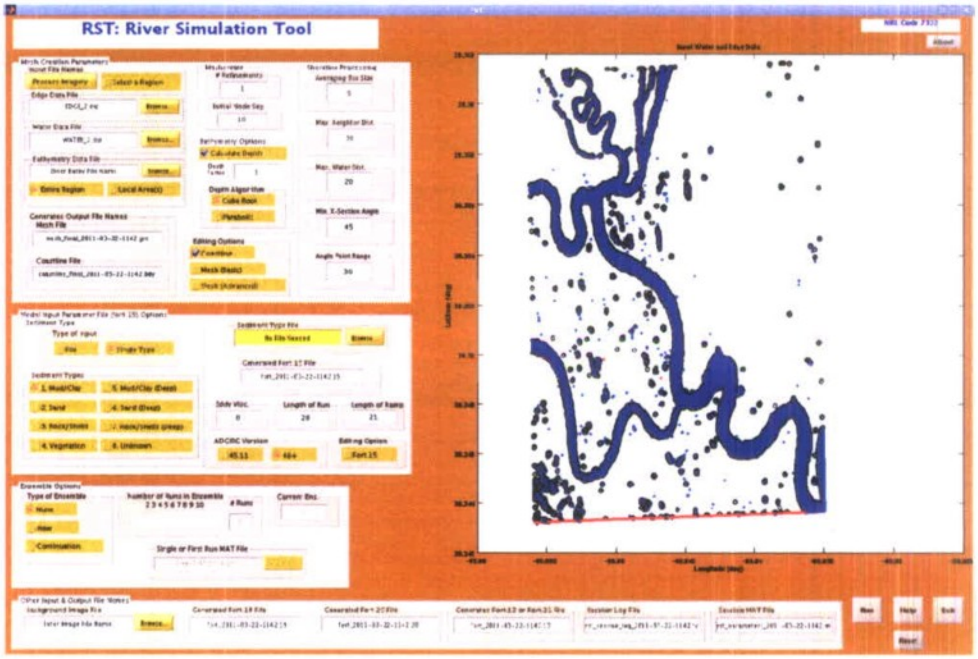

Figure 8. The Graphical User Interface (GUI) for the River Simulation Tool (RST).

At present the RST targets the finite element-based hydrodynamic simulator ADCIRC, the Advanced Circulation Model for Shelves, Coastal Seas, and Estuaries.[6] As such the RST produces model files in formats that directly interface with the ADCIRC model.[13] The grid generation process produces unstructured meshes composed of linear triangles and the specification of forcing and parameter values are also consistent with the ADCIRC model. Future work is aimed toward the creation of additional interfaces within the RST for other hydrodynamic river models.

5. VALIDATION OF SIMULATED SNOHOMISH RIVER CURRENTS

Selection of the Snohomish River as a validation site for the RST and an imagery-initiated model was predicated on the availability of measured bathymetry and observed currents. The final field campaign of the Coherent Structures in Rivers and Estuaries Experiment (COHSTREX) project (sponsored by the Office of Naval Research) deployed five bottom mounted ADCPs from 8-25 September 2009 to record river currents.[3] The measurements were made at three sites within a 2.5 km stretch of the river located approximately 15 km upstream from the mouth. The distance upstream was chosen in order to minimize the influence of stratification. The specific stretch of river was chosen because of the proximity of a variety of bathymetric features. The moorings furthest north are labeled A1, then A2. Site B includes moorings B1, B2, and B3 moving west to east respectively (all moorings are shown in Fig. 9).

The RST-configured river model was executed for two-months starting 1 Aug and ending 31 Oct 2009. A 21-day ramp-up period is imposed to allow the gradual imposition of the forcing. Courant stability limitations govern the selection of a model time step equal to 0.4 sec. Hourly water levels and currents are recorded at every computational point in the mesh while at the five ADCP locations 10-minute data is saved. Fig. 10 depicts

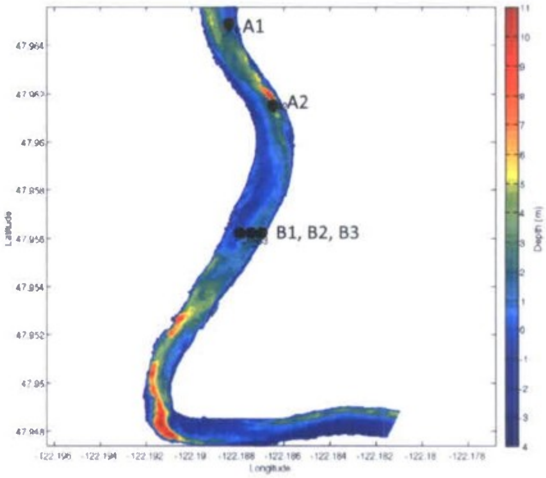

Figure 9. Measured bathymetry and locations of five ADCP moorings for a 8-25 September 2009 field experiment on the Snohomish River, WA.

the current magnitude and direction on 19 Sep 2009 at 14:39 hrs GMT. Overall velocities show a strong tidal influence with maximum currents less than 1 m/s. There is a strong neap/spring variability as well as enhanced currents during the first two days of the analysis period, likely a result of the very large initial upstream discharge conditions.

The modeled currents (depth-averaged) are compared to the observed currents (depth-averaged) in Fig. 11 for the time period of the observations, 8-25 September 2009. The largest discrepancies occur early in the time series during the period of highest discharge. Flows during this time likely exceed the banks of the river, a situation not accounted for in the current image processing approach. The edge and water pixel extractions from the imagery are dependent on flood conditions in the river at the time the image was taken. The extracted shoreline of the river then defines the bounds of the computational model and at present no overflow of the banks is permitted. For a more quantitative comparison, the mean difference error and the mean correlation coefficient at each mooring for current magnitude is presented in Table 1. For the model using the measured bathymetry, correlation coefficients are greater than 85% indicating that the computed currents agree quite well with the observed currents. The difference in magnitude between the computed and observed currents is between 16 and 17 cm/s and remains fairly consistent across all mooring locations.

To evaluate the influence of the synthetic bathymetry on computed currents, an identical river model simulation is repeated now using the RST-generated bathymetry. The measured bathymetry and the synthetic bathymetry are plotted side-by-side in Fig. 12. The synthetic bathymetry is more uniform and symmetric with the thalweg located in the center of the channel, whereas the true bathymetry reflects shoaling on the inside of meander bends and scour (deepening) along the outer edge of the meanders. Error values for currents from the synthetic bathymetry case are also recorded in Table 1. When compared to the observed currents, mean current errors for the synthetic bathymetry case have increased at all mooring locations, an unsurprising result. The large error at mooring A1 is clearly due to the presence of a shoal on the right bank that is not reflected in the synthetic bathymetry. Again, the moorings at B transect the region of sediment accretion along the inner bend of the meander creating a greater discrepancy with the synthetic bathymetry profile. What is surprising

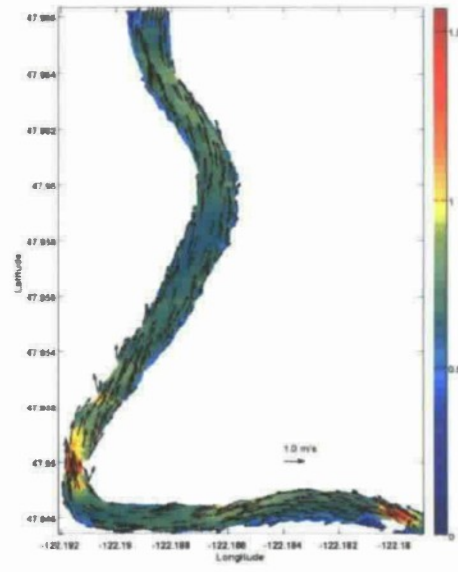

Figure 10. Computed depth-averaged currents for 19 September 2009 14:39 hrs GMT. Magnitude (color) and direction (arrows).

Table 1. Mean error for computed depth-averaged current magnitude at the observational moorings for models using measured and synthetically generated bathymetry.

	Measured Bathymetry		Synthetic Bathymetry	
Mooring	Mean Difference (cm/s)	Correlation	Mean Difference (cm/s)	Correlation
A1	16	0.90	27	0.77
A2	17	0.86	21	0.86
B1	17	0.87	24	0.86
B2	17	0.89	24	0.90
B3	16	0.87	23	0.87

is that mean differences between the computed and observed currents tend to be uniform (about 7 cm/s) across the moorings. Correlation coefficients for currents remain high and quite similar to those recorded for the true bathymetry case. This is an indication that the bathymetry errors have not created large phase differences in the tidal signal. Rather peak currents are damped over the measured currents due to deeper waters generated by the synthetic bathymetry.

6. SUMMARY

An approach has been developed to process river geometry extracted from aerial and satellite imagery. The extracted water and river edge pixel location are used to construct a computational grid a river model. The methodology is fully automated and independent of the imagery source. Additional software, the River Simulation Tool, is developed to provide a simplified interface for river model configuration. The RST, using the river geometry derived from imagery, aims to automate as much of the river model set-up as possible including creation of the computational grid, generation of a synthetic bathymetry if none is available, and the specification of forcing and model parameters with only limited user input required. The methodology and tools described

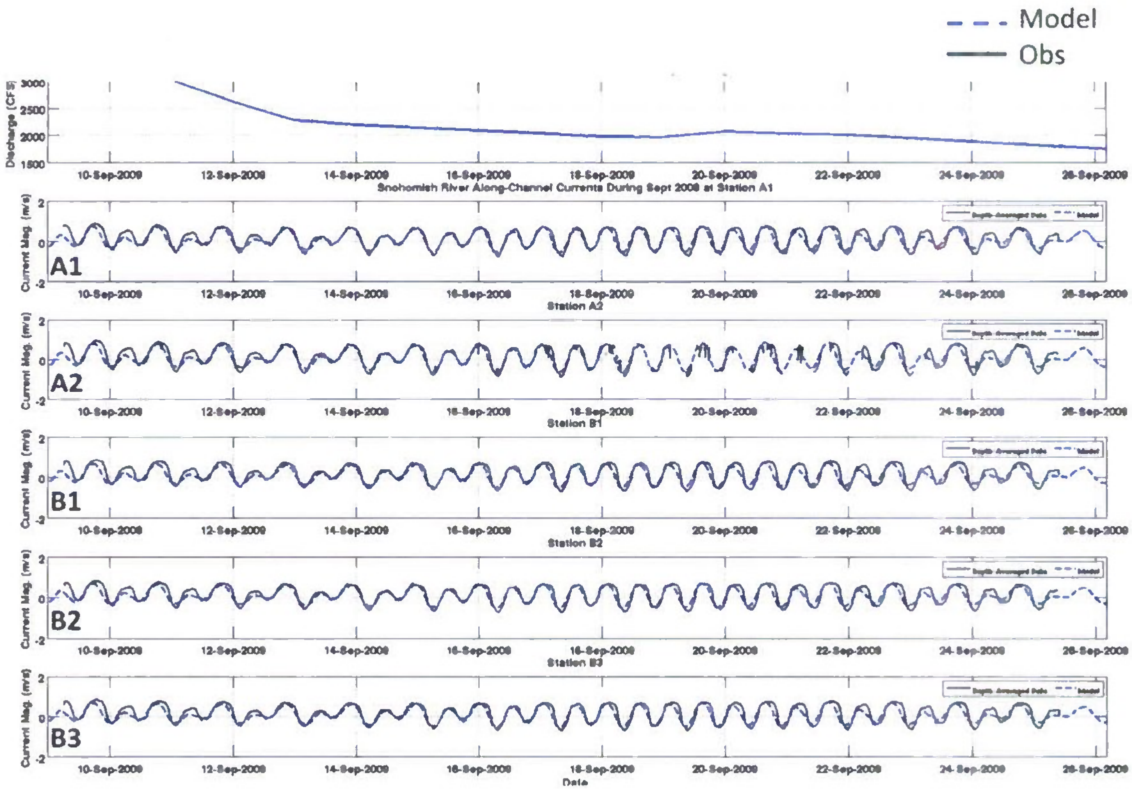

Figure 11. Depth-averaged currents modeled (dashed blue) and observed (solid black) along the Snohomish River from 8-25 Sep 2009.

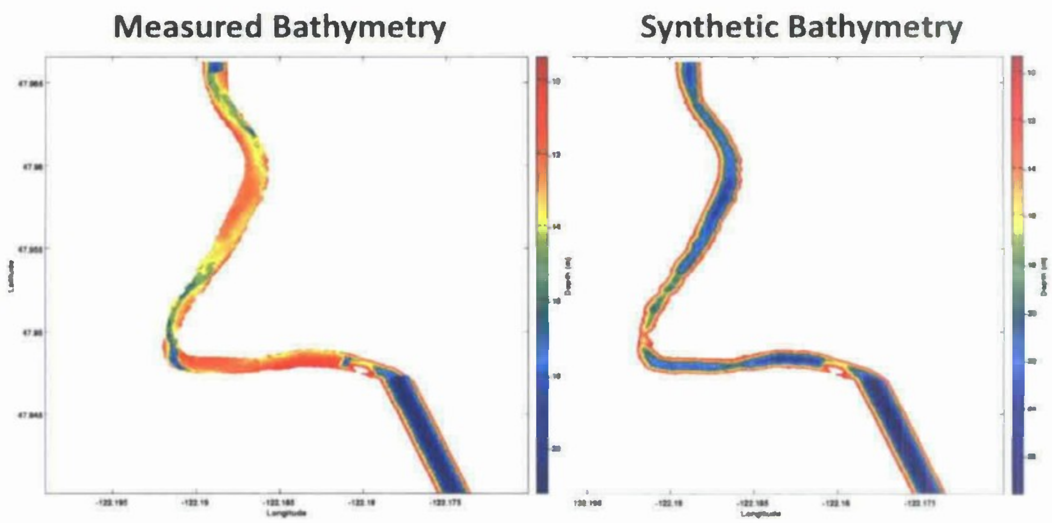

Figure 12. Measured (left) and synthetic (right) bathymetry along the Snohomish River reach.

have been applied here to a reach of the Snohomish River, WA for the purpose of predicting river currents. Computed river currents are compared to observed currents at five locations for an 18-day period in September 2009. Excellent agreement between the computed and observed currents is achieved when the river model utilizes available measured bathymetry. Degraded but reasonable currents are produced by the model when the synthetic bathymetry, available through the RST, is applied. The RST continues to be refined as new river applications are undertaken.

ACKNOWLEDGEMENTS

The authors thank the ONR COHSTREX investigators Andy Jessup, Derek Fong, and C. Chris Chickadel for the use of measured bathymetry and moored current observations taken on the Snohomish River in September of 2009. This work is supported under the NRL 6.2 Core Project "The Performance of a Persistent Riverine Surveillance Network". This paper is NRL contribution number NRL/PP/7320–11-661.

REFERENCES

[1] Lyon, P., "User Manual nitf_warper v1.3.0," (July 2009).

[2] McKay, P., Blain, C. A., and Linzell, R., "Automated identification of rivers and shoreline in aerial imagery using image texture," in [*Proceedings of SPIE, Defense, Security, and Sensing Symposium*], (2011).

[3] Jessup, A. T., Street, R. L., Monismith, S. G., and Horner-Devine, A. R., "Remote Sensing and Modeling of Coherent Structures in River and Estuarine Flows." online (September 2009).

[4] Plant, W. J., Branch, R., Chatham, G., Chickadel, C. C., Hayes, K., Hayworth, B., Horner-Devine, A., Jessup, A., Fong, D. A., Fringer, O. B., Giddings, S. N., Monismith, S., and Wang, B., "Remotely sensed river surface features compared with modeling and in situ measurements," *Journal of Geophysical Research* **C114**, C11002 (2009).

[5] Giddings, S. N., Fong, D. A., and Monismith, S. G., "Role of straining and advection in the intratidal evolution of stratification, vertical mixing, and longitudinal dispersion of a shallow, macrotidal, salt wedge estuary," *Journal of Geophysical Research* **C116**, C03003 (2011).

[6] Luettich, Jr., R. and Westerink, J. J., "Formulation and numerical implementation of the 2D/3D ADCIRC finite element model version 44.XX," (2004).

[7] Luettich, Jr., R., Westerink, J. J., and Scheffner, N. W., "ADCIRC: An advanced three-dimensional circulation model for shelves, coasts, and estuaries, Report 1, Theory and methodology of ADCIRC-2DDI and ADCIRC-3DL," Dredging Research Program Technical Report DRP-92-6, U.S. Army Engineers Waterways Experiment Station, Vicksburg, MS (Nov. 1992). 137p.

[8] Blain, C. A., Linzell, R. S., and Massey, T. C., "MeshGUI: A mesh generation and editing toolset for the ADCIRC model," Tech. Rep. NRL/MR/7322–08-9083, Naval Research Laboratory, Stennis Space Center, MS (February 2008).

[9] Lyard, F., Lefevre, F., Letellier, T., and Francis, O., "Modelling the global ocean tides: Modern insights from FES2004," *Ocean Dynamics* **56**(5-6), 395–415 (2006).

[10] Abdelrhman, M. A., "Simplified modeling of flushing and residence times in 42 embayments in New England, USA, with special attention to Greenwich Bay, Rhode Island," *Estuarine, Coastal and Shelf Science* **62 (1-2)**, 339–351 (2005).

[11] Ward, A. D. and Trimble, S. W., [*Environmental Hydrology*], Lewis Publishers, 2nd ed. (2004).

[12] Blain, C. A., Linzell, R. S., Weidemann, A., and Lyon, P., "A Tool for Rapid Configuration of a River Model," in [*MTS/IEEE Biloxi - Marine Technology for Our Future: Global and Local Challenges*], 1–8, OCEANS 2009 (26-29 Octobert 2009). Marine technolgy Society.

[13] "ADCIRC User's Manual v45." http://www.adcirc.org.